

**Dielectric response in proteins: The proteotronics approach**E. Alfinito<sup>1</sup> and M. Beccaria<sup>2,3</sup>

<sup>1</sup>*Dipartimento di Matematica e Fisica "Ennio De Giorgi", Università del Salento, Lecce, Italy*

<sup>2</sup>*Dipartimento di Matematica e Fisica "Ennio De Giorgi", Università del Salento, Lecce, Italy.*

<sup>3</sup>*National Institute for Nuclear Physics, INFN, Sezione di Lecce, Lecce, Italy*

(\*Electronic mail: [eleonora.alfinito@unisalento.it](mailto:eleonora.alfinito@unisalento.it))

(Dated: 24 February 2026)

The dielectric properties of proteins, particularly in their hydrated state, have been extensively studied. Numerous theoretical and experimental investigations have reported values of both the permittivity and the intrinsic dipole moments of specific proteins under well-defined hydration conditions. Since even approximate estimates of these properties are relevant from both fundamental and applied perspectives, we propose a user-friendly method to calculate the relative permittivity that can be readily integrated into proteotronics workflows. To validate the proposed approach, we compare the results with those obtained using a classical macroscopic method. The outcomes are consistent and contribute further insight into this long-debated issue.

The dielectric response of bulk materials under small applied fields and steady-state conditions is well described within the framework of classical electrodynamics. Classical formulations account for both electronic and intrinsic (orientational) polarization and are independent of the material's shape and size. In contrast, in nanostructured materials the dielectric response is strongly influenced by geometrical factors, including shape and size<sup>1,2</sup>. This aspect is particularly relevant for proteins, *i.e.*, macromolecules characterized by highly irregular, non-geometric shapes, whose structure and functionality are stabilized in the hydrated state<sup>3</sup>.

Proteins are composed of amino acids arranged in a linear sequence referred to as the primary structure. Through the folding process, this sequence adopts a specific three-dimensional conformation corresponding to the native state (tertiary structure). This native conformation is conserved among proteins of the same type and, more broadly, within the same family<sup>4</sup>. The solvent environment plays a crucial role in both the formation and stabilization of the native structure. In particular, water molecules located at the protein surface and within internal cavities provide electrostatic screening of the electric fields generated by charged and polar residues. Their ability to dynamically reorient in response to these fields contributes significantly to conformational stability. In conditions of insufficient hydration, proteins may lose their functional native state and eventually undergo denaturation. The overall dielectric response of a protein, including the orientation and fluctuations of its dipole moment, strongly depends on the surrounding solvent and, more specifically, on the degree of hydration<sup>5–10</sup>.

At the beginning of the 20th century, some seminal papers<sup>11–14</sup> began to investigate the significance of permittivity in dense polar materials. These studies laid the foundation for analyzing the dielectric response of both polar and nonpolar substances in polar environments, initially through analytical approaches<sup>15,16</sup> and later using computational methods<sup>17,18</sup>. Most subsequent investigations of proteins in solution build upon and adapt the Tanford–Kirkwood framework<sup>15,16</sup>. This model distinguishes an internal region of the protein, effectively shielded from solvent effects, and an external region in direct contact with the solvent. The relative dimensions of these regions largely determine the protein's effective dielectric constant<sup>5–7</sup>.

These computational approaches, including molecular dynamics (MD) and Monte Carlo (MC) simulations, are known to be time-consuming, and the results obtained do not always agree with the limited available experimental data. To address this complexity, coarse-grained methods have been developed more recently, based on a continuous distribution of dielectric permittivity within the protein<sup>19,20</sup>. The central idea of this approach is to provide an effective description of the

protein–solvent system: in surface regions and internal cavities, the effective permittivity is taken as an average between water and the protein residues, while within the protein core it approaches the permittivity of the dry residues. A key challenge is determining how to generate this spatial distribution. In the literature, this is often achieved by representing the protein as an equivalent sphere and continuously distributing permittivity values among its amino acids or atoms, based on measures such as the radius of gyration<sup>19</sup>. However, this approach can yield inconclusive results for highly elongated proteins<sup>19</sup>.

Alternatively, we propose evaluating the effective permittivity by considering the number of nearest neighbors for each amino acid. This quantity is a key descriptor of the topological features of a protein’s specific conformation. Specifically, it is used to produce the protein representations through complex networks in a procedure is called proteotronics<sup>21</sup>. Furthermore, it is commonly used to generate two-dimensional representations of the tertiary structure, such as contact maps. Based on this approach, permittivity values are assigned so that highly connected regions correspond to lower permittivity, while less connected regions are assigned higher values. This strategy provides a more accurate estimate of buried versus exposed regions, thereby addressing limitations reported in previous studies<sup>19</sup>.

To define nearest neighbors, we model the protein as a complex network in which nodes correspond to the centroids of amino acids<sup>21–23</sup>. For each node, nearest neighbors are defined as those nodes located within a distance less than  $R_C$ , the interaction radius. The choice of  $R_C$  determines the number of nearest neighbors: very small values ( $< 4 \text{ \AA}$ ) produce a disconnected network, where most nodes have only 0–1 neighbors, whereas very large values result in a fully connected network, with each amino acid linked to all others<sup>21,22,24</sup>. Neither of these extremes is of interest. In this study, we set  $R_C = 6 \text{ \AA}$  which captures the geometric regularity of proteins<sup>6,23,24</sup> and yields an average of approximately five nearest neighbors per node. Tests performed for  $R_C$  values in the range 5–7  $\text{\AA}$  show no qualitative differences in the observed trends.

Finally, an appropriate distribution function must be selected. In principle, different choices may lead to significantly different outcomes. To address this issue, we evaluated several candidate functions, seeking those that yield higher permittivity values for elongated proteins while ensuring consistency across structurally similar proteins. These functions are formulated using nearest-neighbor descriptors, including the maximum value ( $L_{\max}$ ) and the mean value ( $\langle L \rangle$ ) computed over the entire protein.

The test functions are employed to assign a local permittivity value,  $\varepsilon(n)$ , to each  $n$ -th amino

acid.<sup>25</sup> This quantity depends on both the intrinsic (dry) permittivity,  $\epsilon_i(n)$ , and the amino acid’s position within the native protein structure. More specifically,  $\epsilon(n)$  varies between a maximum value corresponding to that of the solvent under standard temperature and pressure (STP) conditions and  $\epsilon_i(n)$ , determined as described in Appendix B. We use three quite standard test functions, namely, linear, sigmoidal and exponential, whose

sharpness can be tuned via a control parameter (Appendix A). Increasing the sharpness enhances the contrast between regions characterized by high and low permittivity, facilitating the identification of hydrated (“wet”) regions associated with larger  $\epsilon(n)$  values. The distinction between an internal low-permittivity region and an external high-permittivity region underlies many theoretical and computational studies<sup>5–7,10</sup>, as the effective dielectric response critically depends on this partitioning.

Finally, the equivalent permittivity of the protein is defined as  $k = \langle \epsilon(n) \rangle$ , i.e., the average of the local permittivity values over all amino acids. This quantity depends on the specific choice of the test function and on its sharpness. Consequently, the control parameters can, in principle, be adjusted to reproduce available experimental data. More importantly, however, the proposed procedure should capture the expected trends in  $k$ . In particular,  $k$  is expected to assume lower values for compact, approximately spherical proteins and higher values for elongated structures, while remaining comparable across proteins with similar conformations.

For this reason, in this Letter we analyze a dataset consisting of 31 proteins, including both single-chain and complex structures, selected to span a range of shapes and sizes and to perform different functions. The aim is to assess whether the proposed approach satisfies the minimal consistency requirements discussed above. The protein selection is arbitrary and may be extended in future studies. Figure 1 presents the normalized permittivity values,  $(k - \langle k \rangle) / \sigma$ , where  $\langle k \rangle$  denotes the mean and  $\sigma$  the standard deviation computed over the dataset. The set of test functions considered captures the differences between elongated and approximately spherical proteins. In particular, elongated proteins systematically exhibit higher average permittivity values than spherical structures.

All test functions show a comparable trend, which suggests that it is not the chosen function itself that is important, but rather the permittivity distribution based on the coordination number. For illustration, Fig. 1 reports the dataset-averaged permittivity obtained using the linear distribution function, shown separately for elongated and spherical proteins.

Finally, we compare previous results with those obtained using a macroscopic approach based

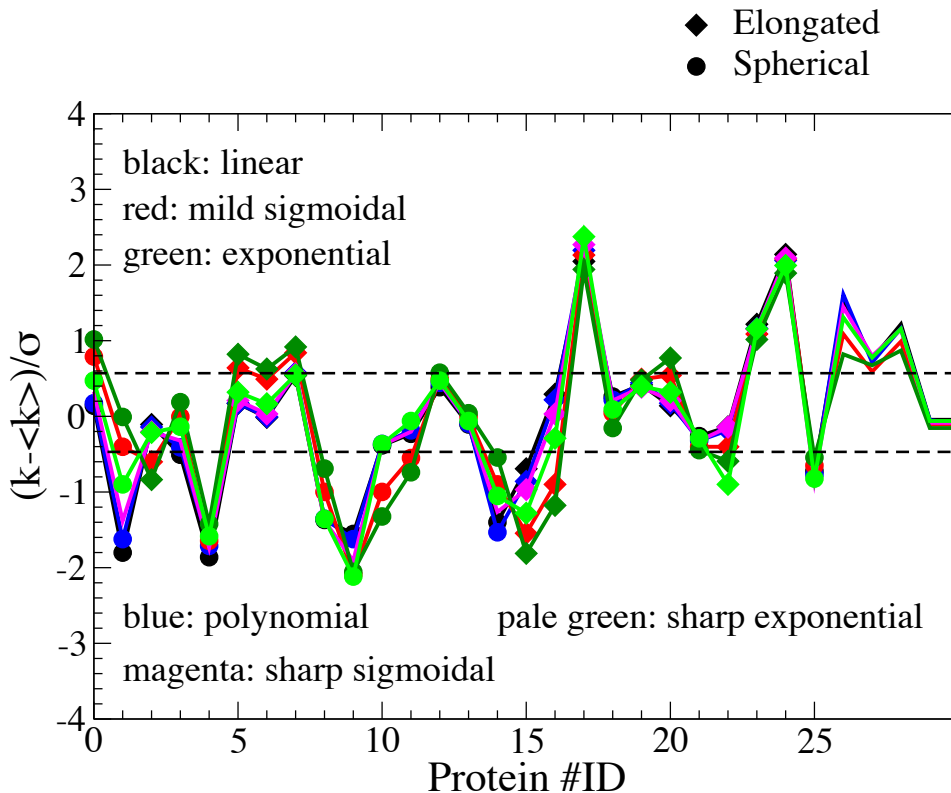


FIG. 1. Normalized effective permittivity,  $k$ , for the selected dataset. The calculation is performed using three test functions (linear, sigmoidal, and exponential). Proteins with different geometrical characteristics (approximately spherical and elongated) are indicated by distinct symbols (dots and diamonds, respectively). Solid lines serve as guides to the eye. Dashed lines denote the mean values for spherical (lower) and elongated (upper) proteins. The complete protein dataset is listed in Table I.

on the evaluation of the protein's electric dipole moment. This analysis is supported by the Protein Dipole Moment Server<sup>26</sup>, developed by Felder, Prilusky, and Sussman, which provides dipole moment estimates for a large number of protein structures available in the Protein Data Bank (PDB)<sup>27</sup>.

Within the framework of classical electrodynamics, the electrical polarizability of a collection of weakly interacting dipoles is determined by the ensemble-averaged dipole orientation induced by an external electric field,  $E$ . The derivation follows from the thermal angular distribution function describing dipole orientations

$$\mathcal{P}(T) d \cos \theta = \frac{e^{-U/k_B T} dU}{\int e^{-U/k_B T} dU}, \quad U = -\mathbf{p}_0 \cdot \mathbf{E} = -p_0 E \cos \theta, \quad (1)$$

where  $k_B$  is the Boltzmann constant, and  $\mathbf{p}_0$  the dipole momentum vector. The mean projection of dipole momentum is

$$\langle p^{\parallel}(T) \rangle = \int p_0 \cos \theta \mathcal{P}(T) d \cos \theta, \quad (2)$$

where  $p^{\parallel} = p_0 \cos \theta$  denotes the component of the intrinsic dipole moment parallel to the applied electric field, i.e., the only component contributing to field screening. In the weak-field limit, the polarizability describes the macroscopic response of the dipole ensemble to the applied field. It is defined in terms of the mean dipole orientation per unit volume:

$$\Pi_0 = n \langle p^{\parallel}(T) \rangle = n \frac{E p_0^2}{3k_B T} \equiv \epsilon_0 \chi_0 E, \quad (3)$$

where  $n$  is the ensemble density.

The susceptibility due to intrinsic dipole orientation is thus

$$\chi_0 = n \frac{p_0^2}{3\epsilon_0 k_B T}. \quad (4)$$

Hydrated proteins cannot be regarded as freely rotating entities, as the surrounding solvent constrains their orientation in the presence of both external and internal electric fields. The native structure itself arises from hydration effects and results from the folding process, which typically positions hydrophilic residues toward the solvent-exposed exterior and hydrophobic residues within the protein core. Water molecules near the surface dynamically reorient in response to local electrostatic fields, thereby reducing the internal electric field generated by charged and polar residues and contributing to structural stability. Consequently, the dipole moment reported in Ref. 26 reflects this solvent-mediated charge organization. In contrast, the dipole moment of the dry protein differs due to the absence of solvent-induced polarization and screening effects.

The dipole moment of a dry protein, denoted as  $p_0$ , can be estimated following the approach proposed by Song<sup>28</sup>. In that paper, the intrinsic polarizabilities of amino acids in proteins were evaluated using molecular dynamics simulations. The term intrinsic refers to a condition in which the dipole moment of each amino acid is assumed to be unaffected by external influences (e.g., solvent effects) and by interactions with other dipoles within the protein<sup>28</sup>. This approximation corresponds to the limiting case of a dry protein, where the dipole moments of individual amino acids are sufficiently small to be considered nearly independent, and solvent-induced polarization is absent. Within this framework, the relative dielectric constant of a protein can be evaluated as  $k_0 = \langle \epsilon(n) \rangle$ , where, for each amino acid,  $\epsilon(n) = \epsilon_i$ , i.e., the intrinsic dielectric constant obtained from Ref. 28 (see Appendix B). The resulting value of  $k_0$  is more or less the same across the

selected proteins, say,  $k_0 \approx 1.5$ , in fine agreement with the outcomes of Ref. 6 (see also Appendix B for details).

A collection of dry proteins may be regarded as freely orientable in an external electric field, due to the absence of solvent-induced friction. Consequently, the dielectric response of the system, *i.e.*, the dry susceptibility,  $\chi_0$ , can be described by Eq. 4. Recognizing that the dipole moment of a hydrated protein,  $p$ , depends on the corresponding dry dipole moment  $p_0$ , the expectation value of polarization under hydrated conditions can be evaluated following Eq. (2). In particular:

$$\langle p^{\parallel}(T) \rangle = \int p \cos \theta \mathcal{P}_0(T) d \cos \theta. \quad (5)$$

We therefore introduce an *effective* susceptibility,  $\chi^H$ , representing the maximal dielectric response of a hydrated protein (cf. Eq. 4):

$$\chi^H = \frac{P p_0}{3 \epsilon_0 \Omega k_B T}. \quad (6)$$

Here,  $n = 1/\Omega$ , with  $\Omega$  denoting the volume of the hydrated protein. Expressing  $p_0$  in terms of the dry susceptibility,  $\chi_0$ , (*cf.* Eq.4) and the dry protein volume,  $\Omega_0$ , the effective susceptibility becomes:

$$\chi^H = \frac{P \sqrt{\chi_0 \Omega_0}}{\sqrt{3 \epsilon_0 k_B T} \Omega}. \quad (7)$$

Finally, we consider the following assumptions: (1) experimental studies indicate no significant differences between the volumes of hydrated,  $\Omega$ , and dry,  $\Omega_0$ , proteins<sup>29</sup>; and (2) the dry susceptibility,  $\chi_0 = k_0 - 1$ , is taken to be approximately constant across different proteins. Under these approximations, Eq. 7 reduces to

$$\chi^H \approx \frac{P}{\sqrt{6 \epsilon_0 \Omega k_B T}}, \quad (8)$$

where  $\chi_0 \approx 0.5$  has been assumed, as previously explained.

In the present analysis, the hydrated protein volume is approximated as  $\Omega = N_{aa} \langle \Omega_{res} \rangle$ , where  $N_{aa}$  denotes the number of amino acids and  $\langle \Omega_{res} \rangle$  is the mean residue volume. The latter is taken as  $127 \text{ \AA}^3$  as in Ref. 30. This estimate is consistent with previous determinations reported in Ref. 31. As a final remark, Eq. 8 yields susceptibility values within the range typically reported for hydrated proteins<sup>6</sup>, *cf.* Tab.I. In contrast, the standard expression,

$$\chi = \frac{p^2}{3 \epsilon_0 \Omega k_B T}, \quad (9)$$

produces values that deviate significantly from this range, *cf.* Tab.I. Finally, we compare the equivalent macroscopic permittivity,  $k^H = \chi^H + 1$ , say,  $(p - p_0)$  model, obtained by Eq. 8 together

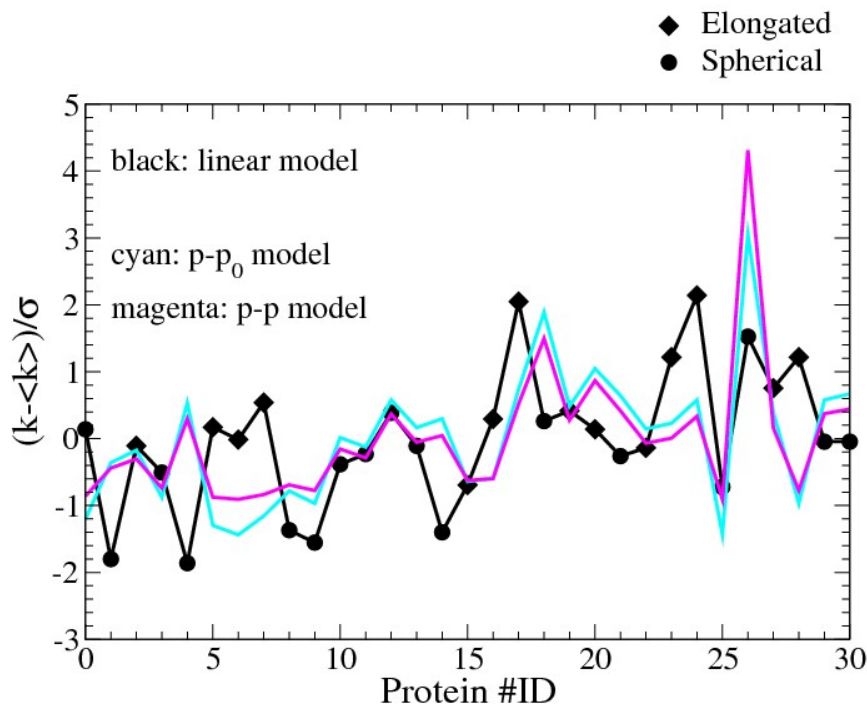


FIG. 2. Normalized *macroscopic* susceptibility for the selected dataset: role of the solvent. The normalized permittivity values obtained using Eq. 6 (the  $p - p_0$  model, cyan solid line) and Eq. 9 (the  $p - p$  model, magenta line) are compared with those calculated using the linear test function (black line).

with dipole moment data from Ref. 26, with permittivity obtained from the continuous microscopic models. Both data are normalized as in Fig.1. The comparison indicates qualitative consistency. In particular, Fig. 2 shows the normalized permittivity calculated using the linear distribution function alongside the macroscopic estimate. The agreement is satisfactory enough, especially for larger proteins ( $ID > 10$ , corresponding to  $N_{aa} > 130$ ). A further comparison using the standard macroscopic dielectric constant derived from Eq. 9 (the  $(p - p)$  model) also shows comparable qualitative agreement.

Finally, we note that Eq. 8, yields an effective macroscopic susceptibility scaling as  $\chi^H \propto p\Omega^{-n} \equiv \chi^H(n)$ , with  $n = 1/2$ . To assess whether the choice  $n = 1/2$  optimizes the agreement with the continuous microscopic models, Fig. 3 compares the previously introduced linear model with  $\chi^H(n)$  evaluated for  $n = 0, 0.5$ , and 1. Within the adopted approximations, the closest agreement is observed for  $n = 1/2$ .

In conclusion, the calculation and definition of permittivity in proteins remain subjects of on-

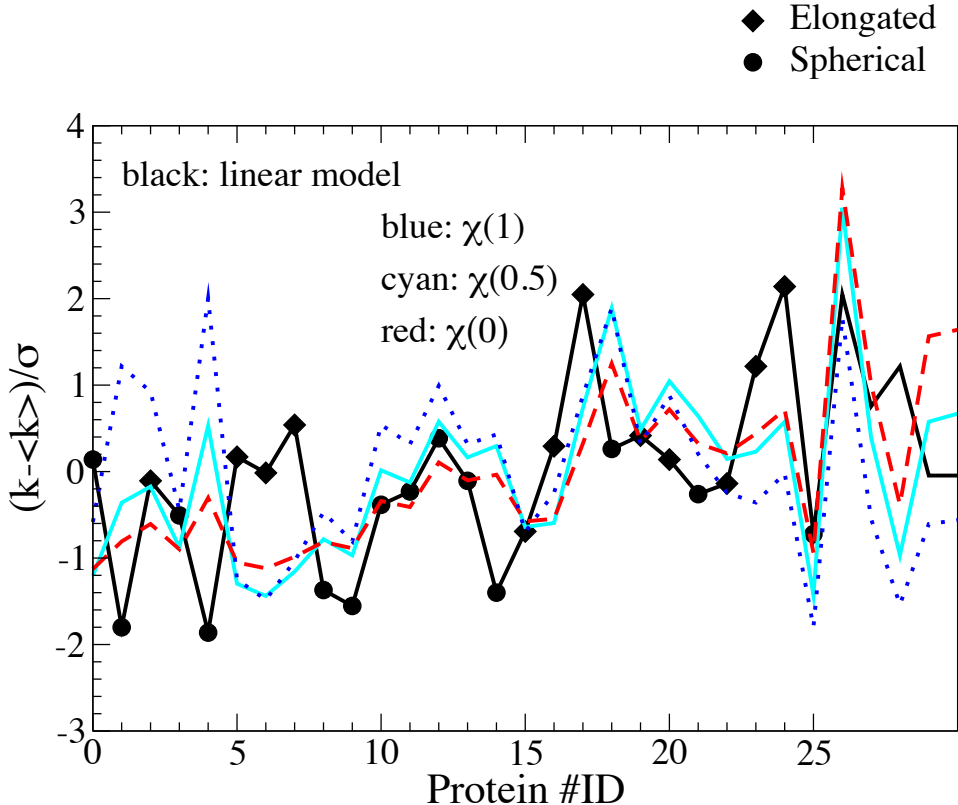


FIG. 3. Normalized *macroscopic* susceptibility for the selected dataset: role of volume. The normalized permittivity values obtained using three different power-law scalings ( $\chi \propto \Omega^{-n}$ , with  $n = 0, 0.5,$  and  $1$ ) are compared with those calculated using the linear test function (black line); see also the main text.

going debate and are known to depend sensitively on the adopted theoretical and computational framework (see, *e.g.*, Ref. 10). In this paper, we propose a computationally efficient and user-friendly approach for estimating the effective macroscopic susceptibility of hydrated proteins. This formulation is motivated by the need to describe the orientational response of macromolecules with restricted rotational mobility arising from their interaction with a polar solvent. The proposed procedure is not intended to provide a complete or fully rigorous description. Rather, it offers a practical strategy that may complement more detailed molecular dynamics approaches, which, despite their accuracy, have not yet produced a comprehensive reference dataset of dielectric properties across diverse protein classes.

In summary, within classical electrodynamics, a system of freely rotating dipoles yields the susceptibility given by Eq. 3. This expression is not directly applicable to hydrated proteins (dipole

moment  $p$ ), as it leads to susceptibility values significantly larger than those reported experimentally (see Table I). The discrepancy arises from the fact that proteins in aqueous environments are not freely orientable: their rotational dynamics are constrained by solvent interactions, which in turn limit their dielectric response. By contrast, the susceptibility evaluated using Eq. 8 produces values qualitatively consistent with the expected range<sup>6</sup>(see Table I). Furthermore, the susceptibility associated with dry proteins (dipole moment  $p_0$ ), denoted as  $\chi_0$ , falls within the range typically attributed to the internal regions of proteins<sup>6</sup>. We emphasize that the difference between  $p$  and  $p_0$  does not primarily originate from structural modifications of the three-dimensional conformation, but rather from changes in polarizability. The dipole moment  $p$  characterizes a hydrated protein, where interfacial water molecules dynamically reorient and influence the distribution of surface charges, thereby altering the dielectric response, particularly for solvent-exposed residues. In contrast,  $p_0$  corresponds to the limiting case of a dry protein, in which the native structure is ideally preserved while solvent-induced polarization and screening effects are absent. Within this interpretation,  $p$  represents a hydration-dependent state derived from  $p_0$ , where the dominant variation concerns the effective permittivity. Accordingly,  $p$  may be regarded as a function of  $p_0$ , and its expectation value can be estimated using the orientational probability distribution associated with the freely rotating dipole  $p_0$ . The results obtained using the two independent procedures show qualitative consistency, supporting the validity of the proposed framework. Nevertheless, further refinements are possible, particularly regarding the selection of test functions, the choice of the interaction radius,  $R_C$  and the evaluation of dipole moments. Finally, we note that in physiological and experimental conditions proteins are generally not freely mobile. This observation suggests that additional investigation is warranted to clarify the definition and interpretation of electrical susceptibility in constrained biological environments.

## AUTHOR DECLARATIONS

### **Conflict of Interests**

The Authors have no conflict of interest to disclose.

### **Author Contribution**

E.A and M.B contributed equally to this paper.

### **Data Availability**

The data that support the findings of this paper are available from the corresponding author upon reasonable request.

## REFERENCES

- <sup>1</sup>C.-m. Mo, L. Zhang, and G. Wang, “Characteristics of dielectric behavior in nanostructured materials,” *Nanostructured Materials* **6**, 823–826 (1995).
- <sup>2</sup>E. Riande and R. Díaz-Calleja, *Electrical properties of polymers* (CRC Press, 2004).
- <sup>3</sup>M.-C. Bellissent-Funel, A. Hassanali, M. Havenith, R. Henchman, P. Pohl, F. Sterpone, D. Van Der Spoel, Y. Xu, and A. E. Garcia, “Water determines the structure and dynamics of proteins,” *Chemical reviews* **116**, 7673–7697 (2016).
- <sup>4</sup>D. Donnelly and J. B. Findlay, “Seven-helix receptors: structure and modelling,” *Current Opinion in Structural Biology* **4**, 582–589 (1994).
- <sup>5</sup>T. Simonson and C. L. Brooks, “Charge screening and the dielectric constant of proteins: insights from molecular dynamics,” *Journal of the American Chemical Society* **118**, 8452–8458 (1996).
- <sup>6</sup>T. Simonson, “Electrostatics and dynamics of proteins,” *Reports on Progress in Physics* **66**, 737 (2003).
- <sup>7</sup>T. Simonson, “Dielectric relaxation in proteins: the computational perspective,” *Photosynthesis research* **97**, 21–32 (2008).
- <sup>8</sup>C. N. Schutz and A. Warshel, “What are the dielectric “constants” of proteins and how to validate electrostatic models?” *Proteins: Structure, Function, and Bioinformatics* **44**, 400–417 (2001).
- <sup>9</sup>Y. Y. Sham, I. Muegge, and A. Warshel, “The effect of protein relaxation on charge-charge interactions and dielectric constants of proteins,” *Biophysical Journal* **74**, 1744–1753 (1998).
- <sup>10</sup>A. Warshel, P. K. Sharma, M. Kato, and W. W. Parson, “Modeling electrostatic effects in proteins,” *Biochimica et Biophysica Acta (BBA)-Proteins and Proteomics* **1764**, 1647–1676 (2006).
- <sup>11</sup>L. Onsager, “Electric moments of molecules in liquids,” *Journal of the American Chemical Society* **58**, 1486–1493 (1936).
- <sup>12</sup>J. G. Kirkwood, “Statistical mechanics of liquid solutions.” *Chemical Reviews* **19**, 275–307 (1936).
- <sup>13</sup>J. G. Kirkwood, “The dielectric polarization of polar liquids,” *The Journal of Chemical Physics* **7**, 911–919 (1939).
- <sup>14</sup>H. Frolich, “Theory of dielectrics, clarendon,” (1949).
- <sup>15</sup>C. Tanford, “The location of electrostatic charges in kirkwood’s model of organic ions,” *Journal of the American Chemical Society* **79**, 5348–5352 (1957).

- <sup>16</sup>C. Tanford and J. G. Kirkwood, “Theory of protein titration curves. i. general equations for impenetrable spheres,” *Journal of the American Chemical Society* **79**, 5333–5339 (1957).
- <sup>17</sup>J. Antosiewicz, “Computation of the dipole moments of proteins,” *Biophysical journal* **69**, 1344–1354 (1995).
- <sup>18</sup>J. J. Havranek and P. B. Harbury, “Tanford–kirkwood electrostatics for protein modeling,” *Proceedings of the National Academy of Sciences* **96**, 11145–11150 (1999).
- <sup>19</sup>L. Li, C. Li, Z. Zhang, and E. Alexov, “On the dielectric “constant” of proteins: smooth dielectric function for macromolecular modeling and its implementation in delphi,” *Journal of chemical theory and computation* **9**, 2126–2136 (2013).
- <sup>20</sup>J. A. Grant, B. T. Pickup, and A. Nicholls, “A smooth permittivity function for poisson–boltzmann solvation methods,” *Journal of computational chemistry* **22**, 608–640 (2001).
- <sup>21</sup>E. Alfinito, L. Reggiani, and J. Pousset, “Proteotronics: Electronic devices based on proteins,” in *Sensors: Proceedings of the Second National Conference on Sensors, Rome 19-21 February, 2014* (Springer, 2015) pp. 3–7.
- <sup>22</sup>E. Alfinito, J.-F. Millithaler, L. Reggiani, N. Zine, and N. Jaffrezic-Renault, “Human olfactory receptor 17-40 as an active part of a nanobiosensor: a microscopic investigation of its electrical properties,” *Rsc Advances* **1**, 123–127 (2011).
- <sup>23</sup>E. Alfinito, J.-F. Millithaler, C. Pennetta, and L. Reggiani, “A single protein based nanobiosensor for odorant recognition,” *Microelectronics journal* **41**, 718–722 (2010).
- <sup>24</sup>E. Alfinito, C. Pennetta, and L. Reggiani, “A network model to correlate conformational change and the impedance spectrum of singleproteins,” *Nanotechnology* **19**, 065202 (2008).
- <sup>25</sup>Hereafter, the term permittivity refers to the relative permittivity, i.e., the permittivity normalized to the vacuum permittivity.
- <sup>26</sup>C. E. Felder, J. Prilusky, I. Silman, and J. L. Sussman, “A server and database for dipole moments of proteins,” *Nucleic acids research* **35**, W512–W521 (2007).
- <sup>27</sup>H. M. Berman, J. Westbrook, Z. Feng, G. Gilliland, T. N. Bhat, H. Weissig, I. N. Shindyalov, and P. E. Bourne, “The protein data bank,” *Nucleic acids research* **28**, 235–242 (2000).
- <sup>28</sup>X. Song, “An inhomogeneous model of protein dielectric properties: Intrinsic polarizabilities of amino acids,” *The Journal of chemical physics* **116**, 9359–9363 (2002).
- <sup>29</sup>Y. Harpaz, M. Gerstein, and C. Chothia, “Volume changes on protein folding,” *Structure* **2**, 641–649 (1994).
- <sup>30</sup>M. Amin and J. Küpper, “Variations in proteins dielectric constants,” *ChemistryOpen* **9**, 691–694

(2020).

<sup>31</sup>C. R. Chen and G. I. Makhatadze, “Proteinvolume: calculating molecular van der waals and void volumes in proteins,” *BMC bioinformatics* **16**, 101 (2015).

<sup>32</sup>F. Cardarelli, *Materials handbook: a concise desktop reference* (Springer, 2008).

<sup>33</sup>“2020-09-17 jimmy eng. uw proteomics resource,” <http://www.umimod.org/masses.html> (2020).

## Appendix A: Model function

Within the proteotronics framework, each protein conformation is represented as an interaction network in which nodes correspond to amino acids centroids<sup>22-24</sup>. Links between nodes are introduced when the inter-residue distance is smaller than a prescribed interaction radius,  $R_C$ , taken here as 6 Å. Under this construction, each node is characterized by a coordination number, i.e., the number of nearest neighbors, which depends on its position within the network. Model distribution functions are employed to assign a local dielectric constant,  $\varepsilon(n)$ , to the  $n$ th amino acid. This parameter varies between the intrinsic value  $\varepsilon_i(n)$ <sup>28</sup> and  $\mu$ , representing the dielectric permittivity of the solvent.

**Model 1:** polynomial

$$\varepsilon(n) = \varepsilon_i(n)x^m(n) + \mu(1 - x^m(n)), \quad (\text{A1})$$

**Model 2:** sigmoidal

$$\begin{aligned} \varepsilon(n) &= \varepsilon_i(n)x(n)w + \mu(1 - x(n))(1 - w), \\ w &= \frac{L^q(n)}{L^q(n) + \langle L \rangle^q}. \end{aligned} \quad (\text{A2})$$

**Model 3:** exponential

$$\varepsilon(n) = \varepsilon_i(n)x(n) + \mu(1 - x(n)) \exp \left[ - \left( \frac{L(n)}{\langle L \rangle} \right)^q \right], \quad (\text{A3})$$

with  $x(n) = \frac{L(n)}{L_{\max}}$ , where  $L(n)$  denotes the coordination number associated with the  $n$ th amino acid,  $L_{\max}$  is the maximum coordination number observed among all amino acids in the protein and  $\langle L \rangle$  is the average value.

In all models, the parameters  $q$  and  $m$  control the sharpness of the function and, consequently, the spatial extent of the region where  $\varepsilon(n)$  assumes its largest values. From a physical standpoint,

## Dielectric response in proteins

these parameters effectively describe the degree of protein hydration. In the present work, the three models are implemented using two distinct parameter sets, specifically:

Model 1:  $m = 1, 0.5$  (linear and polynomial);

Model 2:  $q = 1, 6$  (mild and sharp sigmoidal)

Model 3:  $q = 1, 6$  (mild and sharp exponential)

## Appendix B: Tables

Table I summarizes, for the analyzed protein dataset, the dipole moment  $p$  obtained from Ref. 26, the effective susceptibilities of hydrated ( $\chi^H$ ) and dry ( $\chi_0$ ) proteins, and the dipole moment of the dry protein,  $p_0$ , as estimated in this Letter. Dipole moments are expressed in debye (D).

The intrinsic permittivity, of each amino acid,  $\epsilon_i$ , is evaluated using the Clausius–Mossotti relation together with the molecular polarizabilities,  $\alpha$ , reported in Ref. 28. Specifically,

$$\frac{4n\pi\alpha}{3} = \frac{\epsilon_i - 1}{\epsilon_i + 2}, \quad (\text{B1})$$

where  $n = \rho \mathcal{N}_A / A$ , with  $\mathcal{N}_A$  denoting Avogadro’s number,  $\rho$  the molecular density<sup>32</sup>, and  $A$  the mass number<sup>33</sup>.

All data are resumed in Table II.

## ACKNOWLEDGMENTS

We thank Professors Joel Sussman and Jaime Prilusky (Weizmann Institute of Science, Rehovot, Israel) for helpful discussions regarding the Protein Dipole Moment Server.

This paper has been partially funded by the Italian MUR project GINEVRA, prot. 2022BZYBWM.

## Dielectric response in proteins

TABLE I. List of proteins used in this paper. Dipole values are given in debyes. Notice that for complex proteins like 1p9m, 2gy7,2j8c both whole structure (biological unit) and single chains -(protein<sub>chain</sub>)- are reported.

ID	<sup>a</sup> Code	$N_{aa}$	<sup>b</sup> $p$ (D)	<sup>c</sup> $\chi^H$	$p_0$ (D)	$\chi_0$
0	1c09	53	74	6	6	0.48
1	1c9o	66	200	15	6	0.65
2	1uz3	102	280	17	8	0.56
3	1brk	108	164	10	8	0.62
4	1bkr	108	400	24	8	0.62
5	1nzt	128	104	6	9	0.65
6	1aiz	129	77	4	9	0.59
7	1e65	129	130	7	9	0.66
8	3lzt	129	198	11	9	0.60
9	1b0b	141	169	9	9	0.55
10	1alu	157	385	19	10	0.72
11	1p9m <sub>B</sub>	163	358	17	10	0.72
12	1p9m <sub>C</sub>	201	562	25	11	0.70
13	1z3s	216	480	20	12	0.65
14	2gy7 <sub>A</sub>	216	506	21	12	0.65
15	2ntw	222	292	12	12	0.37
16	2ntu	222	304	13	12	0.37
17	2j8c <sub>H</sub>	241	649	26	12	0.49
18	2j8c <sub>L</sub>	281	1015	38	13	0.42
19	1p9m <sub>A</sub>	298	660	24	14	0.63
20	1n26	299	805	29	14	0.70
21	2j8c <sub>M</sub>	302	649	23	14	0.47
22	1u19	348	604	20	15	0.50
23	2gy7 <sub>B</sub>	423	694	21	16	0.55
24	2gy5	423	804	24	16	0.55
25	3ehs	457	148	4	17	0.55
26	2ace	527	1819	49	18	0.56
27	2gy7	639	959	23	20	0.58
28	1p9m	662	368	9	20	0.58

## Dielectric response in proteins

TABLE II. List of main data used for the calculation of intrinsic dielectric constant  $\epsilon_i$

amino acid	<sup>a</sup> $A$	<sup>b</sup> $\rho(\text{g}/\text{\AA}^3)$	<sup>c</sup> $n(\text{mol}/\text{\AA}^3)$	<sup>d</sup> $\alpha(\text{\AA}^3)$	$\epsilon_i$
alanine	71	1.430	$1.12 \times 10^{-2}$	1.1	1.18
arginine	156	1.230	$0.47 \times 10^{-2}$	5.7	1.38
asparagine	114	1.543	$0.82 \times 10^{-2}$	9.8	2.51
aspartic acid	115	1.700	$0.89 \times 10^{-2}$	4.0	1.52
cysteine	103	1.180	$0.69 \times 10^{-2}$	1.8	1.16
glutamic acid	129	1.538	$0.72 \times 10^{-2}$	6.2	1.69
glutamine	128	1.364	$0.64 \times 10^{-2}$	17.7	3.72
glycine	57	1.161	$1.23 \times 10^{-2}$	2.2	1.38
histidine	137	1.309	$0.57 \times 10^{-2}$	12.3	2.26
isoleucine	113	1.293	$0.69 \times 10^{-2}$	1.1	1.10
leucine	113	1.293	$0.69 \times 10^{-2}$	1.2	1.11
lysine	128	1.136	$0.53 \times 10^{-2}$	8.4	1.70
methionine	131	1.178	$0.54 \times 10^{-2}$	2.8	1.20
phenylalanine	147	1.160	$0.47 \times 10^{-2}$	1.0	1.06
proline	97	1.180	$0.73 \times 10^{-2}$	1.3	1.12
serine	87	1.600	$1.11 \times 10^{-2}$	7.3	2.54
threonine	101	1.131	$0.67 \times 10^{-2}$	8.2	1.90
tryptophan	186	1.175	$0.38 \times 10^{-2}$	1.8	1.09
tyrosine	163	1.237	$0.46 \times 10^{-2}$	5.3	1.34
valine	99	1.230	$0.75 \times 10^{-2}$	1.0	1.10

<sup>a</sup> mass number: <http://www.unimod.org/masses.html>, 2025-09-24 Jimmy Eng, UW Proteomics Resource

<sup>b</sup> <https://matmake.com/properties/density-of-amino-acids.html>

<sup>c</sup> Ref. 32

<sup>d</sup> Ref. 28